# Photoinduced nucleation theory in one-dimensional systems

Kazuki Koshino*
*Department of Physics, Tohoku University, Aoba-ku, Sendai 980-8578, Japan*
*and Institute of Physics, University of Tokyo, 3-8-1 Komaba, Tokyo 153-8902, Japan*

Tetsuo Ogawa†
*Department of Physics, Tohoku University, Aoba-ku, Sendai 980-8578, Japan*
*and ''Structure and Transformation,'' PRESTO, Japan Science and Technology Corporation (JST), Sendai 980-8578, Japan*
(Received 8 June 1998)

Photoinduced nucleation of a kink-antikink pair in a one-dimensional system is investigated theoretically, using a model composed of localized two-level electrons and classical lattices, which has two structural phases. We treat the case of the finite-ranged intersite interaction, in order to discuss the crossover from short-ranged to long-ranged interaction. In particular, we focused on the structural change induced by a one-site photoexcitation. When a single site is excited, a local structural change is created around the excited site at first. After the emission of a photon from the excited site, this local structural change (a) remains local, (b) grows into a kink-antikink pair, or (c) disappears and the system returns to the initial phase. Nucleation of a kink-antikink pair occurs only when the intersite interaction is short ranged and moderately strong. The motion of the kinks is also examined. [S0163-1829(98)03046-X]

## I. INTRODUCTION

Nucleation of critical droplets in a metastable phase has been attracting much attention in both physics and chemistry.[1] In one-dimensional systems, the critical droplet has the form of a kink-antikink pair, and its physical properties are investigated based on the models such as the kinetic Ising model, the reaction-diffusion equation, and so on.[2,3] In these works, the trigger for nucleation is attributed to the thermal fluctuations, and nucleation of a critical droplet occurs when a large enough fluctuating force to get over the activation energy is applied to the system.

The critical droplets, however, are not nucleated only by the thermal fluctuations. There exist some materials where the first-order phase transition can be induced by irradiation of light. For example, in polydiacetylene single crystals, a structural phase transition can be induced with a single shot of a pulsed laser between the blue and red phases with different bond structures.[4] In order to treat such photoinduced phenomena theoretically, it is indispensable to take into account of the electronic excited states as well as the ground state, and the interaction with the photons. Recently, we have presented some of the main results of such a theory.[5]

The aim of the present paper is to discuss in detail the photoinduced nucleation of kink-antikink pairs in the one-dimensional system, using a model which contains the electronic degrees of freedom. The model describes a structural phase transition between the two locally stable structural phases, where the structural change is brought about by the relaxation after photoexcitation of the system. The structural change after *one-site* excitation by a photon is examined in particular, to find out the condition under which the one-site excitation can nucleate a kink-antikink pair.

This paper is organized as follows. We introduce in Sec. II a one-dimensional system composed of localized electrons and lattice distortions, which has two locally stable structures. In Sec. III, we discuss the properties of the individual sites by neglecting the intersite interaction, and show the condition for a site to possess two locally stable structures. We also discuss the local structural change in a single site, which occurs through three different processes. The structural change induced by one-site excitation by a photon is examined in Sec. IV, stressing the role of the intersite coupling, and the condition for inducing the structural phase transition by a single photon is clarified. The dynamics of the structural phase transition, which takes the form of the propagation of the kinks, is discussed in Sec. V. The finite-temperature effects on the photoinduced structural change are discussed in Sec. VI.

## II. MODEL

### A. Hamiltonian

As the minimal model for the photoinduced cooperative structural changes, we investigate a one-dimensional system, each site of which is composed of a two-level localized electron and a lattice distortion.[5–7] The state of a single site is specified by the distortion $\tilde{u}_j$ of the lattice (see Fig. 1), which we treat classically, and the wave function $|\phi\rangle_j$ of the localized electron, which we assume to be a linear combination of two states $|1\rangle_j$ and $|2\rangle_j$. The Hamiltonian for this system has the following form:

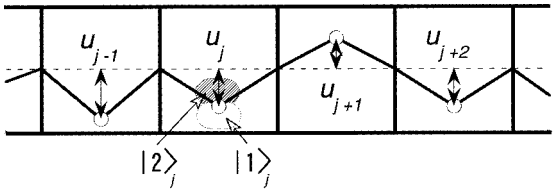


FIG. 1. Schematic view of the one-dimensional system considered in this paper.

 

$$\tilde{\mathcal{H}}=\sum_j \left[ \tilde{\mathcal{H}}_j^e+\frac{\tilde{k}_0}{2}\tilde{u}_j^2+\frac{\tilde{M}}{2}\left(\frac{d\tilde{u}_j}{d\tilde{\tau}}\right)^2 \right] \tag{2.1}$$

$$+\sum_{(i,j)} \frac{\tilde{k}_{ij}}{2}(\tilde{u}_i-\tilde{u}_j)^2, \tag{2.2}$$

where $\tilde{k}_0$ and $\tilde{k}_{ij}$ are the elastic constants, and $\tilde{M}$ is the mass of the lattice. The summation in Eq. (2.2) runs over $i$ and $j$ satisfying $i>j$. The last term (2.2) represents the intersite interaction, which decreases the differences in the distortions. $\tilde{\mathcal{H}}_j^e$ is a single-site electronic Hamiltonian, which operates on the $j$th localized electronic wave function $|\phi\rangle_j$,

$$\tilde{\mathcal{H}}_j^e=\begin{pmatrix} \tilde{\epsilon}-\tilde{\gamma}_1\tilde{u}_j & \tilde{t} \\ \tilde{t} & \tilde{\gamma}_2\tilde{u}_j \end{pmatrix}, \tag{2.3}$$

where $\tilde{\epsilon}$ denotes the energy difference between the two electronic state $|1\rangle_j$ and $|2\rangle_j$ at $\tilde{u}_j=0$, $\tilde{t}$ the overlap integral between them, $\tilde{\gamma}_1$ and $\tilde{\gamma}_2$ the electron-lattice coupling constants.

Though not explicitly shown in the Hamiltonian, the system is coupled to the reservoir, composed of other phonon modes, photon fields, and so on. Thus the system is an open system, and therefore the energy of the system does not conserve. This energy dissipation will be introduced phenomenologically later.

Using the characteristic energy $\tilde{\epsilon}_c=\tilde{\gamma}_2^2/2\tilde{k}_0$, length $\tilde{u}_c=\tilde{\gamma}_2/\tilde{k}_0$, and frequency $\tilde{\Omega}_c=(2\tilde{\epsilon}_c/\tilde{M}\tilde{u}_c^2)^{1/2}$, we can rewrite the Hamiltonian $\mathcal{H}=\tilde{\mathcal{H}}/\tilde{\epsilon}_c$ in the following dimensionless form:

$$\mathcal{H}=\sum_j \left[ \mathcal{H}_j^e+u_j^2+\left(\frac{\partial u_j}{\partial \tau}\right)^2 \right] \tag{2.4}$$

$$+\sum_{(i,j)} k_{ij}(u_i-u_j)^2, \tag{2.5}$$

$$\mathcal{H}_j^e=\begin{pmatrix} \epsilon-2\gamma u_j & t \\ t & 2u_j \end{pmatrix}, \tag{2.6}$$

where $u_j=\tilde{u}_j/\tilde{u}_c$, $\epsilon=\tilde{\epsilon}/\tilde{\epsilon}_c$, $t=\tilde{t}/\tilde{\epsilon}_c$, $\gamma=\tilde{\gamma}_1/\tilde{\gamma}_2$, $k_{ij}=\tilde{k}_{ij}/\tilde{k}_0$, and $\tau=\tilde{\tau}\tilde{\Omega}_c$. Those variables without tildes are dimensionless.

### B. Adiabatic approximation

Throughout this paper, we apply the adiabatic approximation to this system. It is valid when the nonadiabatic transition can be neglected, i.e., the motion of the lattices is slow enough. By estimating the typical velocity of the lattice at $\tilde{u}_c\tilde{\Omega}_c$, the condition for this approximation to be valid is represented by

$$t \gtrsim \sqrt{\frac{\tilde{\hbar}\tilde{\Omega}_c}{\tilde{\epsilon}_c}}, \tag{2.7}$$

according to the Landau-Zener theory.[8]

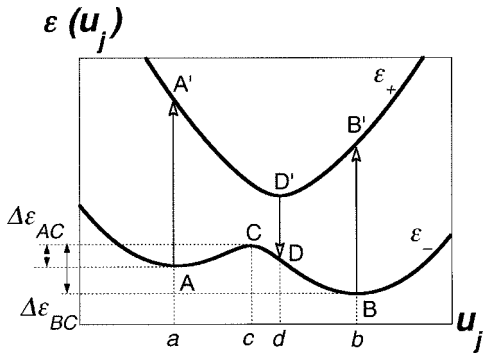


FIG. 2. The adiabatic potential $\epsilon_\pm(u_j)$. The upward (downward) arrow represents the electronic transition with absorption (emission) of a photon. $\Delta\epsilon_{AC}=\epsilon_-(c)-\epsilon_-(a)$ and $\Delta\epsilon_{BC}=\epsilon_-(c)-\epsilon_-(b)$ are the potential barriers.

## III. SINGLE-SITE PROPERTIES

In this section, we discuss the dynamics in a single site, neglecting the intersite interaction Eq. (2.5). Besides the adiabatic motion of the lattice, we introduce the electronic transition between the ground and excited states, which accompanies absorption or emission of a photon. We show that a single site may possess two locally stable structures under an appropriate choice of the single-site parameters $\epsilon$, $\gamma$, and $t$, and that the structural change occurs via three different processes, namely, the optical, thermal, and quantum processes.

### A. Dynamics in a single site

Under the adiabatic approximation, the dynamics in a single site consists of the adiabatic motion of the lattice and the electronic transition between the ground state $|-(u_j)\rangle_j$ and excited state $|+(u_j)\rangle_j$, which are the eigenvectors of the single-site Hamiltonian $\mathcal{H}_j=\mathcal{H}_j^e+u_j^2$. The adiabatic motion of the lattice occurs along the following adiabatic potentials:

$$\epsilon_\pm(u_j)=u_j^2+(1-\gamma)u_j+\frac{\epsilon}{2}\pm\sqrt{\left[\frac{\epsilon}{2}-(1+\gamma)u_j\right]^2+t^2}, \tag{3.1}$$

which are the corresponding eigenvalues. The sign should be chosen according to the electronic state of the site. The shape of these potentials is drawn in Fig. 2. The derivative of $\epsilon_-$ ($\epsilon_+$) becomes zero at $u_j=a,b$, and $c(u_j=d)$. We hereafter call these four structures A, B, C, and D′, respectively.

The equation of motion for the lattice at the $j$th site is

$$\ddot{u}_j=-\frac{\partial}{\partial u_j}\epsilon_\pm(u_j)-\Gamma\dot{u}_j+\eta_j(\tau), \tag{3.2}$$

where $\Gamma$ is the dimensionless friction constant, and $\eta_j$ is the thermal fluctuating force. The last two terms represent the coupling to other phonon modes or reservoir. According to the fluctuation-dissipation theorem,[9] $\Gamma$ and $\eta_j$ are related by $\langle\eta_j(\tau)\eta_j(\tau')\rangle=4\Gamma(\tilde{k}_B\tilde{T}/\tilde{M}\tilde{u}_c^2\tilde{\Omega}_c^2)\delta(\tau-\tau')$, where $\tilde{T}$ is the lattice temperature.

We introduce the dipole transition between the ground and excited states, accompanying absorption or emission of a photon. According to the Franck-Condon principle, the mo-

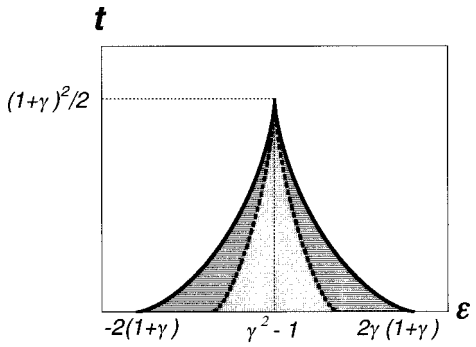


FIG. 3. The single-site parameter region $(\epsilon,t)$ for the system to be bistable (the whole shadowed region) and to possess the possibility of nucleation of the kink-antikink pair by one-site excitation (the hatched regions).

tion of the lattice is negligible during the transition, so the transition is represented by the vertical arrows in Fig. 2. The dipole-transition matrix elements are given in Appendix A.

### B. Stable and metastable structures

We can find three locally stable structures A, B, and D′ in Fig. 2. Among these structures, A and B are stable at zero temperature, while D′ is unstable even at zero temperature because of the radiative decay to D. We regard this system to be bistable with the metastable structure A and the stable structure B.

In fact, for a large value of $\epsilon$ or $t$, the system does not have bistability, i.e., $\epsilon_-$ has only a single minimum. The system can be bistable only with an appropriate choice of the single-site parameters $\epsilon$, $\gamma$, and $t$, as shown in Fig. 3. Because the region where the adiabatic approximation to be valid is given by Eq. (2.7), the following condition:

$$\sqrt{\frac{\tilde{\hbar}\tilde{\Omega}_c}{\tilde{\epsilon}_c}} \ll \frac{(1+\gamma)^2}{2} \sim 1, \tag{3.3}$$

is required, which holds when the motion of the lattice is slow enough.

### C. Processes for the local structural change

The local structural change between A and B occurs through three different processes: the optical, thermal, and quantum processes, as explained in the following.

#### 1. The optical process

The electronic excitation due to absorption of a photon may trigger a structural change as follows. The electronic excitation in the A (B) structure is represented by the vertical line A→A′ (B→B′) in Fig. 2. Then the lattice relaxes to D′ obeying Eq. (3.2) with the plus sign, which finishes within the time of order $\Gamma^{-1}$ ($\Gamma$) when $\Gamma$ is large (small). Because it is usually much smaller than the typical radiative lifetime (by order $10^4$), the electronic transition to the ground state always occurs at $u_j=d$, which is represented by D′→D. After that, the lattice finally relaxes to B obeying Eq. (3.2) with the minus sign.

To summarize, a site in the A structure makes a structural change to B by photoexcitation, while a site in the B structure returns to the initial B structure. We neglect the small probability of relaxing to the opposite structure, for example, due to the nonadiabatic transition B′→A.

#### 2. The thermal process

The thermal fluctuating force may also cause the structural change, which we call the thermal process. This process occurs, contrary to the optical process, only on the potential surface $\epsilon_-$. If the lattice gets a large enough fluctuating force to override the potential barrier $\Delta\epsilon_{\rm AC}$ ($\Delta\epsilon_{\rm BC}$), the thermally induced structural change occurs through the path A→C→B (B→C→A) in Fig. 2. Because the probability to get such large fluctuating force is proportional to the thermal activation factor $\exp(-\Delta\epsilon_{\rm AC}\tilde{\epsilon}_0/\tilde{k}_B\tilde{T})[\exp(-\Delta\epsilon_{\rm BC}\tilde{\epsilon}_0/\tilde{k}_B\tilde{T})]$, the whole system will finally relax to the thermal equilibrium.

#### 3. The quantum process

The site in the A structure can change into the B structure by the quantum tunneling. This process originates from the quantum nature of the lattice, which we neglect in this paper. Because this process occurs independent of the lattice temperature, it becomes important at low temperature instead of the thermal process.

## IV. NUCLEATION OF THE KINK-ANTIKINK PAIRS

In the preceding section, we have briefly summarized the properties of the individual site, neglecting the intersite interaction (2.5). Now we start to investigate the photoinduced nucleation of the kink-antikink pairs in a one-dimensional system, which is a cooperative phenomenon brought about the intersite interaction. Because our main interest lies in the photoinduced dynamics, we consider only the case that the lattice temperature is absolute zero in order to exclude the effect of the thermal fluctuation. As the most simple case of the photoinduced dynamics, we focus on the structural change after *one-site* excitation by a photon.

For simplicity, we hereafter assume that the intersite interaction can be parametrized by the total strength $k$ and the force range $\mu$ as

$$k_{ij}=\frac{k}{2}(1-e^{-1/\mu})\exp\left(-\frac{|i-j|-1}{\mu}\right). \tag{4.1}$$

In the limit of $\mu\to 0$, it approaches the nearest-neighbor interaction $k_{ij}=(k/2)\delta_{|i-j|,1}$, while in the limit of $\mu\to\infty$, it approaches the infinite ranged constant $k_{ij}=k/N$, where $N$ is the total number of the sites.

### A. Relaxation after one-site excitation

Relaxation after one-site excitation proceeds in two steps. First, the system relaxes in the one-site-excited adiabatic potential $E_+^{(1)}$. After the spontaneous emission of a photon from the excited site, the system then starts to relax in the ground-state adiabatic potential $E_-$.

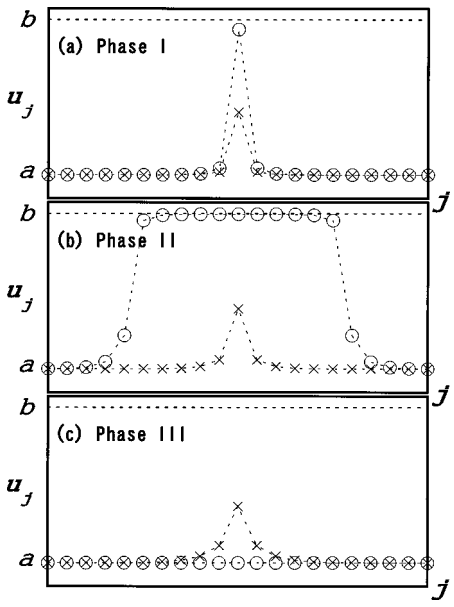


FIG. 4. The real-space configuration of the structural change after one-site excitation with the single-site parameters $\epsilon=-0.5$, $\gamma=1$, $t=1.1$. The interaction range is chosen to be $\mu=0.5$, the interaction strength (a) $k=0.05$, (b) $k=0.2$, (c) $k=0.5$, and the friction $\Gamma=1$. The relaxed positions just before the spontaneous emission ($\{\overline{u_j}\}$) are plotted by crosses and the configurations after the spontaneous emission ($\tau=\tau_{\rm SE}+50$) by open circles.

#### *1. Relaxation before the spontaneous emission*

We consider the case that a single site (e.g., zeroth site) in the A (B) structure is excited by a photon at $\tau=0$. Then, the lattices start to move according to the equations of motion,

$$\ddot{u}_j=-\frac{\partial}{\partial u_j}E_+^{(1)}(\{u_j\})-\Gamma\dot{u}_j \quad (0<\tau<\tau_{\rm SE}), \tag{4.2}$$

where $E_+^{(1)}$ is the one-site-excited adiabatic potential,

$$E_+^{(1)}(\{u_j\})=\sum_{j(\neq 0)}\epsilon_-(u_j)+\epsilon_+(u_0)+\sum_{(i,j)}k_{ij}(u_i-u_j)^2. \tag{4.3}$$

The initial condition is $u_j=a(b)$ for all $j$. The relaxation to the minimum of $E_+^{(1)}$ finishes within the time of order $\Gamma$ ($\Gamma^{-1}$) if the friction constant $\Gamma$ is large (small). The lattices centered around the excited site distort from their initial positions, as shown in Fig. 4 by the cross symbols. We denote these relaxed positions by $\{\overline{u_j}\}$, which is the local minimum point of $E_+^{(1)}$. The approximate form of $\{\overline{u_j}\}$ is presented in Appendix B.

#### *2. Relaxation after the spontaneous emission and appearance of three phases*

The excited site emits a photon spontaneously at $\tau=\tau_{\rm SE}$ (typically $\tau_{\rm SE}\sim 10^4$), which is usually much larger than the time to finish the relaxation described above. Then, the lattices start to move again following the equations of motion:

$$\ddot{u}_j=-\frac{\partial}{\partial u_j}E_-(\{u_j\})-\Gamma\dot{u}_j \quad (\tau_{\rm SE}<\tau), \tag{4.4}$$

where $E_-$ is the ground-state adiabatic potential,

$$E_-(\{u_j\})=\sum_j\epsilon_-(u_j)+\sum_{(i,j)}k_{ij}(u_i-u_j)^2. \tag{4.5}$$

The initial condition at $\tau=\tau_{\rm SE}$ is $\{u_j\}=\{\overline{u_j}\}$.

If the system starts from the A structure at $\tau=0$, we can now observe the following three qualitatively different cases as shown in Fig. 4; (a) only the excited site makes a structural change to B (phase I), (b) every site yields a structural change to B (phase II), and (c) every site goes back to the A structure (phase III).

On the other hand, if the system starts from the B structure at $\tau=0$, every site always goes back to the B structure, i.e., only phase III can be observed. It is because even the excited site can never be distorted largely enough to satisfy $\overline{u_0}<c$ before the spontaneous emission.

### B. Condition for nucleation of a kink-antikink pair

#### *1. Phase diagrams on the $(k,\mu)$ plane*

As shown in Fig. 4, one-site excitation in the metastable A structure results in three qualitatively different cases. The crucial factor for these behaviors is the intersite interaction $k_{ij}$. In Figs. 5(a) and 5(b), the phase diagrams are drawn on the $(\mu,k)$ plane with the single-site parameters $(\epsilon,\gamma,t)$ and the friction constant $(\Gamma)$ fixed, by solving Eqs. (4.2) and (4.4) numerically. The distinct difference between the two diagrams is the existence of phase II, where a global structural change is induced by one-site excitation.

The common feature to both diagrams is that phase I lies in the region of small $k$ and phase III lies in the region of large $k$. This can be understood by simple considerations. In the limit of weak interaction $k\to 0$, every site behaves independently, and according to the foregoing discussion on a single site, only the excited site makes a structural change from A to B. Thus phase I appears in the region of small $k$. On the other hand, in the limit of strong interaction $k\to\infty$, even the excited site cannot be distorted largely enough to satisfy $\overline{u_0}>c$ before the spontaneous emission because of the large cost of the elastic energy. Obviously, every site goes back to A. Thus phase III appears in the region of large $k$.

While phases I and III always appear in the phase diagram regardless of the single-site parameters $(\epsilon,\gamma,t)$, phase II does not appear as in Fig. 5(b), or appears in the region of small $\mu$ and intermediate $k$ as in Fig. 5(a). The fact that phase II appears only when the interaction is short-ranged may seem curious, because long-range interactions are thought to be important in cooperative phenomena generally. The reason is that the region of the B structure extends *step by step through the domino effect*,[5] which can be more effectively induced in the case that the local structural change around the excited site exerts strong influence upon the neighboring sites than in the case that it exerts weak influence upon many remote sites.

#### *2. Two critical interaction strengths*

To understand the phase diagrams (Fig. 5) quantitatively, we introduce two critical interaction strengths $k_1(\mu)$ and $k_2(\mu)$ in the following way.

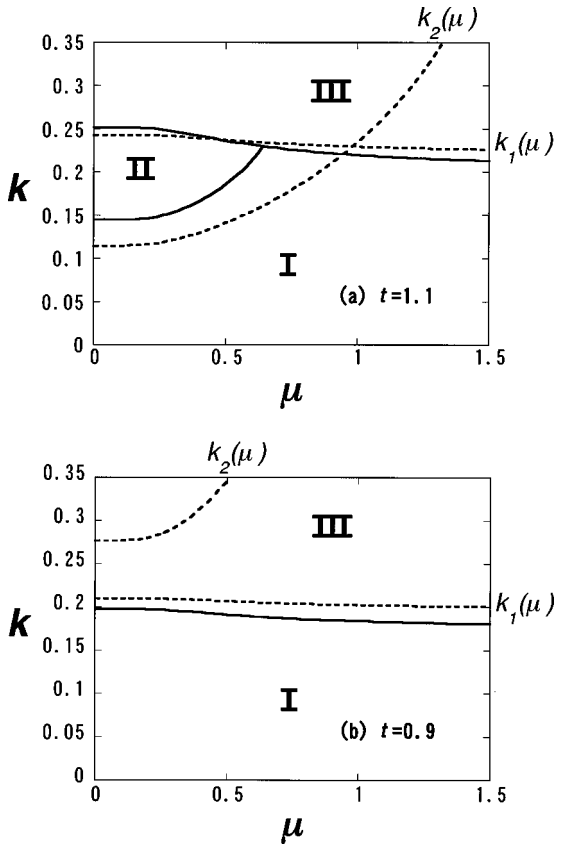


FIG. 5. The phase diagram on the $(\mu,k)$ plane with the single-site parameters (a) $\epsilon=-0.5$, $\gamma=1$, $t=1.1$, (b) $\epsilon=-0.5$, $\gamma=1$, $t=0.9$, and the friction constant $\Gamma=1$. The critical interaction strengths $k_1(\mu)$ and $k_2(\mu)$ are also drawn by broken lines for comparison.

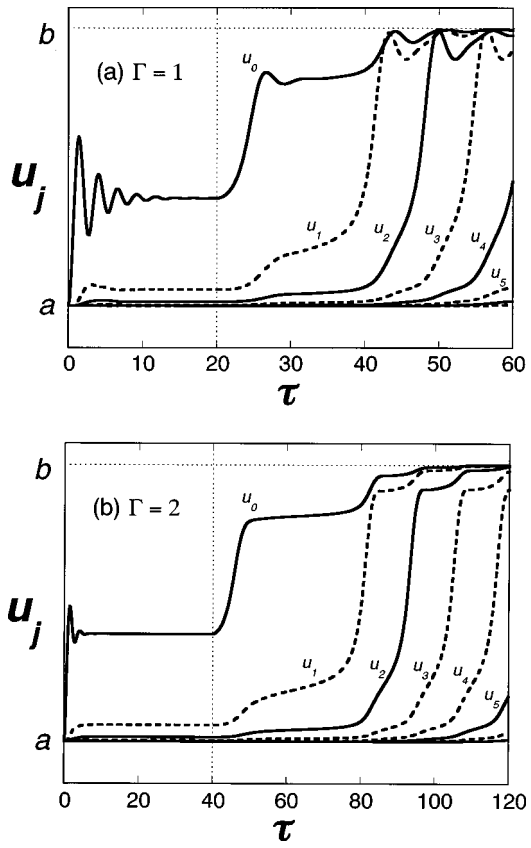


FIG. 6. The domino motion of the sites as a function of time in the case of $\epsilon=-0.5$, $\gamma=1$, $t=1.1$, $k=0.2$, $\mu=0.5$, (a) $\Gamma=1$, and (b) $\Gamma=2$. $\tau_{\mathrm{SE}}$ is set to be (a) 20 and (b) 40.

First, we discuss the possibility of the structural change of the excited site. The motion of the excited site just after the spontaneous emission is determined by $\partial E_-(\{\overline{u_j}\})/\partial u_0$. We define $k_1(\mu)$ as the solution of the following equation:

$$\frac{\partial}{\partial u_0}E_-(\{\overline{u_j}\})=0. \tag{4.6}$$

If $k$ is smaller (larger) than $k_1$, $\partial E_-(\{\overline{u_j}\})/\partial u_0$ is positive (negative) and the lattice moves towards the A (B) structure.

Next, we consider the possibility of the structural changes of the nearest neighbor ($\pm 1$st) sites when the excited (0th) site has changed to B. Instead of solving Eq. (4.4) with Eq. (4.5) exactly, we roughly assume that $u_0$ and $u_j$ $(|j|>1)$ are fixed to $b$ and $a$ while $u_{\pm 1}$ is in motion. Making use of the equality $u_{-1}=u_1$, the effective potential $w_1$ for $u_1$ is given by

$$w_1(u_1)\equiv\epsilon_-(u_1)+\frac{k}{2}(1-e^{-1/\mu})(u_1-b)^2+\frac{k}{2}(1+e^{-2/\mu})\times(u_1-a)^2. \tag{4.7}$$

While $w_1$ has a potential barrier between the A and B structures for small $k$, it disappears for large enough $k$. We define $k_2(\mu)$ as the value of $k$ where the potential barrier disappears. Thus, if $k$ is greater than $k_2$, the structural change of the $\pm 1$st sites are induced by that of the 0th site, and the region of the stable B structure extends through the domino effect. If $k$ is smaller than $k_2$, however, the $\pm 1$st sites only make a slight distortion from the A structure, and the structural change remains local.

Using these two critical strengths of the interaction, phases I, II, and III correspond to $k<\min(k_1,k_2)$, $k_2<k<k_1$, and $k_1<k$, respectively. $k_1(\mu)$ [calculated with Eq. (4.6) and $\{\overline{u_j}\}$ given in the Appendix A] and $k_2(\mu)$ are drawn in Fig. 5, indicating that $k_1$ $(k_2)$ is a decreasing (increasing) function of $\mu$. Thus, if $k_1$ is smaller than $k_2$ at $\mu=0$, phase II does not appear in the phase diagram. It means that phase II appears only under an appropriate choice of the single-site parameters, as shown in Fig. 3. The single-site parameter region where phase II can yield lie along the edge of the region where the system has bistability. In other words, phase II can exist only when the potential barrier $\Delta\epsilon_{\mathrm{AC}}$ is small, i.e., the metastable structural phase is fragile.

## V. MOTION OF THE KINKS

In this section, we investigate the propagation of the kinks in phase II, as shown in Fig. 4(b). In order to visualize the temporal behavior, we show in Figs. 6(a) and 6(b) the temporal motion of the lattices, which indicates that the kink moves at a constant velocity (the domino motion). It should be noted that the equation of motion (4.4) with Eq. (4.5), which describes the motion of the kinks, is basically equivalent to the reaction-diffusion equation, based on which the constant motion of the kinks is concluded.[3] We here present

the estimation of the velocity of the kinks in this discretized model.

We can roughly explain the motion of the lattices observed in Fig. 6 as follows. In the previous section, we have shown that the kink-antikink pair can be nucleated only when the intersite interaction is short-ranged and moderately strong. The width of the kink, which is estimated at $\lambda$ defined by Eq. (B11), is then so small that we can assume $u_{n-1}=u_{n-2}=\cdots=b$ and $u_{n+1}=u_{n+2}=\cdots=a$, while $u_n$ is in motion. This assumption allows us to regard that the $n$th site moves in the following potential $v_n(u_n)$,

$$v_n(u_n)\equiv\epsilon_-(u_n)-\frac{k}{2}[(u_n-a)^2+(u_n-b)^2]. \tag{5.1}$$

$v_n(u_n)$ has a minimum at $u_n=b^*(<b)$, which corresponds to the point at which the lattice stops transiently before reaching $b$.

We regard the time $T$ for the lattice to move from $a$ to $b^*$ as the time for the kink to move for one site. We can easily evaluate the time $T$, because it is a problem of classical mechanics of a single particle following the equation,

$$\ddot{u}_n=-\frac{dv_n}{du_n}-\Gamma\dot{u}_n. \tag{5.2}$$

When $\Gamma$ is large, we can approximate the velocity of the lattice by $\dot{u}_n\sim|v_n'(u_n)|/\Gamma$. Then, the lattice is allowed to move from $a$ to $b^*$ if $v_n'(u_n)<0$ is satisfied for $a<u_n<b^*$, and $T$ is evaluated as

$$T\sim\Gamma\int_a^{b^*}\frac{du_n}{|v_n'(u_n)|}. \tag{5.3}$$

The proportionality to $\Gamma$ can be confirmed by the comparison between Figs. 6(a) and 6(b). $T$ becomes large for large $\Gamma$ and in the neighborhood of $k_2(\mu)$ in the phase diagram Fig. 5.

On the other hand, when $\Gamma$ is small enough to be neglected, we can approximate the velocity of the lattice by $\dot{u}_n\sim\sqrt{2[v_n(a)-v_n(u_n)]}$. Then, the lattice is allowed to move from $a$ to $b^*$ if $v_n(a)>v_n(u_n)$ is satisfied for $u_n>a$, and $T$ is evaluated as

$$T\sim\int_a^{b^*}\frac{du_n}{\sqrt{2[v_n(a)-v_n(u_n)]}}. \tag{5.4}$$

The transition time $T_{\rm tot}$ for the whole system is then given by

$$T_{\rm tot}\sim\tau_{\rm SE}+NT, \tag{5.5}$$

where $N$ is the total number of the sites. For a small system ($NT\ll\tau_{\rm SE}$), $T_{\rm tot}$ is of the order of $\tau_{\rm SE}$ and the dependence on the system size is hidden by the fluctuation of $\tau_{\rm SE}$. On the other hand, for a large system ($NT\gg\tau_{\rm SE}$), the proportionality of $T_{\rm tot}$ to the system size can be revealed.

## VI. DISCUSSION AND CONCLUSIONS

### A. Finite-temperature effects

At a finite temperature, the effect of the thermal noise should be taken into account. An apparent effect is the thermally induced structural change, which is discussed in many papers.[1] We here restrict ourselves to a discussion of the finite-temperature effects only on the *photoinduced* structural change.

We treat the case of $\tilde{k}_B\tilde{T}\ll\tilde{\epsilon}_c$, in order that the metastable state has a long lifetime. At such a low temperature, the thermal electronic excitation can be neglected and only the thermal fluctuation of the lattices should be taken into account. Because of the thermal fluctuation, the excited site fluctuates around $u_0=\overline{u_0}$ with a width

$$\Delta u\sim\left[\frac{2\tilde{k}_B\tilde{T}}{\tilde{\epsilon}_c\epsilon_+''(d)}\right]^{1/2}. \tag{6.1}$$

This makes the curve $k_1(\mu)$ obscure. By utilizing the relation

$$\frac{d\overline{u_0}}{dk}\simeq-2\frac{d-a}{\epsilon_+''(d)}, \tag{6.2}$$

which can be derived by differentiating Eq. (B6) at $k=0$, we can estimate the width $\Delta k_1$ of $k_1(\mu)$ at temperature $\tilde{T}$ as

$$\Delta k_1\simeq\frac{1}{d-a}\sqrt{\frac{\epsilon_+''(d)\tilde{k}_B\tilde{T}}{2\tilde{\epsilon}_c}}. \tag{6.3}$$

The thermal noise also affects the motion of the nearest-neighbor sites. They can change into the B structure even if there is a potential barrier in $w_1(u_1)$ of the height about $\tilde{k}_B\tilde{T}$. This will decrease $k_2(\mu)$ by the value

$$\Delta k_2\simeq\frac{1}{(b-a)^2}\frac{\tilde{k}_B\tilde{T}}{\tilde{\epsilon}_c}, \tag{6.4}$$

at the temperature $\tilde{T}$, using a rough estimate of the height of the potential barrier at $\Delta k_2(a-b)^2$. As a result, the phase diagram at a finite temperature becomes Fig. 7.

### B. Conclusions

To treat the photoinduced nucleation phenomena in one-dimensional system, we proposed a model composed of localized two-level electrons and lattices, which possesses two structural phases.

The dynamics in a single site was discussed at first, neglecting the intersite interaction. Under the adiabatic approximation, it can be described by the adiabatic motion of the lattice and the electronic dipole transition between the two electronic states, accompanying absorption or emission of a photon. The condition for the system to have bistability was presented and three possible processes for the structural change was discussed.

Next, we discussed the nucleation of the kink-antikink pair, including the intersite interaction. In particular, we focused on the structural change induced by a one-site excitation by a photon at zero temperature. The system at first relaxes in the one-site-excited adiabatic potential, and makes a local structural change. After the emission of a photon from the excited site, the system then relaxes in the ground-state adiabatic potential, and the local structural change (a)

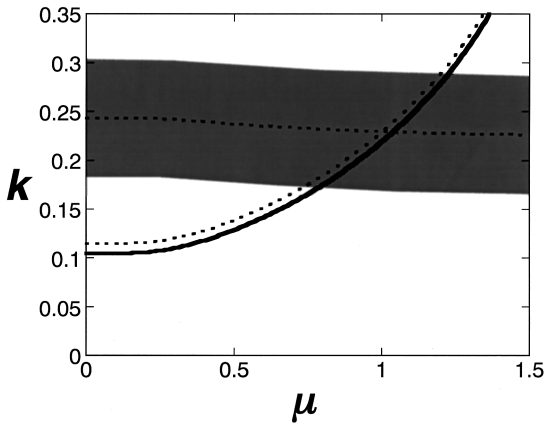


FIG. 7. The schematic phase diagram at a finite temperature ($\tilde{T}=0.01\tilde{\epsilon}_c/\tilde{k}_B$) with the single-site parameters $\epsilon=-0.5$, $\gamma=1$, $t=1.1$. The dotted lines represent $k_1(\mu)$ and $k_2(\mu)$ at zero temperature.

remains local, (b) grows into a kink-antikink pair, or (c) disappears and the system returns to the initial phase, as shown in Fig. 4. If the initial structural phase is the globally stable one, only the case (c) can be observed. On the other hand, if the initial structural phase is the metastable one, those three qualitatively different cases can be observed depending on the strength and the range of the intersite interaction. The condition for the photoinduced nucleation of the kink-antikink pair is (i) the metastable structure is fragile, and (ii) the intersite interaction is short ranged and moderately strong.

Finally, we investigated the motion of the kinks. The kink moves at a constant velocity, which could be estimated by solving a classical mechanics of a single particle. We also touched the finite temperature effects on the photoinduced dynamics.

Throughout this paper, we have applied the adiabatic approximation, assuming that the condition (2.7) is satisfied. When $t$ is very small, however, the lattices should be regarded to move in the *diabatic* potential, and the *nonradiative* process becomes important.[10] We will present a more general theory applicable to the small $t$ case. The role played by the quantum nature of the lattice should also be considered.

## ACKNOWLEDGMENTS

The authors are grateful to S. Koshihara, K. Kitahara, T. Luty, H. Cailleau, and H. Nishimori for stimulating discussion. This work was partly supported by the Grant-in-Aid from the Ministry of Education, Science, Sports, and Culture of Japan.

## APPENDIX A: DIPOLE TRANSITION

The interaction between the localized electron and the electromagnetic field is briefly summarized in this section. We consider only the dipole transition of the form $\tilde{\mu}\tilde{E}$, where $\tilde{E}$ is the electromagnetic field and $\tilde{\mu}$ is the dipole operator for the localized electron,

$$\tilde{\mu}=-\tilde{e}\begin{pmatrix}\tilde{a} & \tilde{b}\\ \tilde{b} & -\tilde{a}\end{pmatrix}, \tag{A1}$$

where $-\tilde{e}$ represents the charge of the electron, and the matrix is the position operator for the electronic wave function. The diagonal elements represent the difference in the position by $2\tilde{a}$ between the two electronic states $|1\rangle_j$ and $|2\rangle_j$, while the off-diagonal elements $\tilde{b}$ represent the usual dipole transition matrix elements. The transition dipole between the excited and ground states is then given by

$$\tilde{\mu}_{\pm}(u_j)=\frac{t}{\sqrt{[\epsilon/2-(1+\gamma)u_j]^2+t^2}}\,\tilde{e}\tilde{a} - \frac{\epsilon/2-(1+\gamma)u_j}{\sqrt{[\epsilon/2-(1+\gamma)u_j]^2+t^2}}\,\tilde{e}\tilde{b}. \tag{A2}$$

The first term dominates when the lattice distortion is around $u_j=\epsilon/2(1+\gamma)$, i.e., $c$ or $d$ in Fig. 2, while the second term dominates when the lattice distortion is far from $u_j=\epsilon/2(1+\gamma)$, i.e., $a$ or $b$ in Fig. 2.

The spontaneous emission rate $\tau_{SE}^{-1}$ of a photon from the excited site also depends on the distortion $u_j$ of the lattice. It is given by

$$\tau_{SE}^{-1}=\frac{\tilde{\epsilon}_c^3|\tilde{\mu}_{\pm}(u_j)|^2}{3\pi\tilde{\epsilon}_0\tilde{\hbar}^4\tilde{c}^3\tilde{\Omega}_c}[\epsilon_+(u_j)-\epsilon_-(u_j)]^3, \tag{A3}$$

where $\tilde{\epsilon}_0$ is the dielectric constant in the vacuum. The typical order of $\tau_{SE}$ is $10^4$, which is usually much larger than the period of the lattice oscillation.

## APPENDIX B: APPROXIMATE FORM OF THE LOCAL DISTORTION

In this section, we show the approximate form of $\{\overline{u_j}\}$, which is the solution of the equation,

$$\frac{\partial}{\partial u_j}E_+^{(1)}(\{\overline{u_j}\})=0, \tag{B1}$$

with the boundary condition $\overline{u_j}=a$ for large $j$. Without the intersite interaction, i.e., $k=0$, the solution of Eq. (B1) is trivial: $\overline{u_j}=a+(d-a)\delta_{j,0}$. We approximate the bottoms of $\epsilon_{\pm}(u_j)$ by the parabolas, and use the following potentials instead:

$$\epsilon_+(u_j)=\epsilon_+(d)+\frac{\epsilon_+''(d)}{2}(u_j-d)^2, \tag{B2}$$

$$\epsilon_-(u_j)=\epsilon_+(a)+\frac{\epsilon_+''(a)}{2}(u_j-a)^2. \tag{B3}$$

Using the ansatz

$$\overline{u_j}=a+\alpha e^{-j/\lambda}, \tag{B4}$$

where $\alpha$ and $\lambda$ are to be determined, we get the following approximate form of $\{\overline{u_j}\}$:

$$\overline{u}_0 = a + \frac{(d-a)(c_{22}-c_{12})}{c_{11}c_{22}-c_{12}c_{21}}, \tag{B5}$$

$$\overline{u}_j = a + \frac{(d-a)(c_{11}-c_{21})}{c_{11}c_{22}-c_{12}c_{21}} e^{-(j-1)/\lambda} \quad (j \neq 0), \tag{B6}$$

where

$$c_{11} = 1, \tag{B7}$$

$$c_{12} = 2\epsilon''_-(a)[(1-e^{-1/\lambda})\epsilon''_+(d)]^{-1}, \tag{B8}$$

$$c_{21} = 1 + 2k/\epsilon''_+(d), \tag{B9}$$

$$c_{22} = -2k(1-e^{-1/\mu})[(1-e^{-1/\lambda-1/\mu})\epsilon''_+(d)]^{-1}. \tag{B10}$$

Here $\lambda$ represents the length of the distorted region (the kink width) given by

$$\lambda^{-1} = \cosh^{-1}\left[ e^{-1/\mu} + \frac{\sinh(1/\mu)}{1+[2+\epsilon''_-(a)/k]^{-1}(e^{1/\mu}-1)} \right]. \tag{B11}$$

*Electronic address: koshino@cmpt01.phys.tohoku.ac.jp
†Electronic address: ogawa@cmpt01.phys.tohoku.ac.jp

[1] P. Hanggi, P. Talkner, and M. Borkovec, Rev. Mod. Phys. **62**, 251 (1990).
[2] T. Christen, Phys. Rev. E **51**, 604 (1995).
[3] M. Buttiker and H. Thomas, Phys. Rev. A **37**, 235 (1988).
[4] S. Koshihara, Y. Tokura, K. Takeda, and T. Koda, Phys. Rev. Lett. **68**, 1148 (1992).
[5] K. Koshino and T. Ogawa, J. Phys. Soc. Jpn. **67**, 2174 (1998).
[6] E. Hanamura and N. Nagaosa, J. Phys. Soc. Jpn. **56**, 2080 (1987).
[7] N. Nagaosa and T. Ogawa, Phys. Rev. B **39**, 4472 (1989).
[8] C. Zener, Proc. R. Soc. London, Ser. A **137**, 696 (1932).
[9] R. Kubo, M. Toda, and N. Hashitsume, *Statistical Physics II* (Springer, Berlin, 1985).
[10] K. Koshino and T. Ogawa (unpublished).